Synthesis of Monodisperse Nanocrystals of Manganese Oxides

2 AUTHORS:

Ming Yin
Columbia University
11 PUBLICATIONS **1,379** CITATIONS

SEE PROFILE

Stephen O'Brien
City College of New York
126 PUBLICATIONS **7,700** CITATIONS

SEE PROFILE

Synthesis of Monodisperse Nanocrystals of Manganese Oxides

Ming Yin and Stephen O'Brien*

*Department of Applied Physics and Applied Mathematics and Materials Research Science and Engineering Center,
Columbia University, New York, New York 10027*

Received May 21, 2003; E-mail: so188@columbia.edu

The magnetic, structural, and transport properties in manganese oxides have attracted considerable interest, driven by a desire to understand their unique properties from a fundamental standpoint.[1] Manganese oxides also find applications in catalysis and battery technologies.[2] MnO is a model system for the theoretical study of electronic and magnetic properties of rock salt oxides,[3,4] and recent experimental studies have shown ferromagnetic behavior in MnO nanoclusters, even though MnO is antiferromagnetic in the bulk.[5] To this end, there is much to be gained from the ability to synthesize highly crystalline, monodisperse nanocrystals of manganese oxides without size selection and with control over morphology.[5-8]

Here, we report the synthesis and characterization of nanocrystals of MnO, capped with organic ligands and highly dispersible in nonpolar solvents. The nanocrystals are relatively monodisperse (>10% rms diameter), and control over the reaction conditions can generate a range of sizes between 7 and 20 nm. The nanocrystals are stable indefinitely under N_2 and stable in air for up to periods of months. Controlled chemical oxidation can allow for the preparation of nanocrystals of Mn_3O_4 from MnO. We also demonstrate the use of simple acetate precursors in the preparation of ligand-capped transition metal nanocrystals (of MnO and FeO), which are safer and more environmentally benign than their metal carbonyl counterparts.[5,6] MnO nanocrystals of length 7 nm were synthesized by thermal decomposition of manganese acetate in the presence of oleic acid at high temperature. The reaction is believed to proceed via decomposition of the acetate to a manganese oxide–oleic acid complex, with the formation of CO_2 and acetone.[9] In a typical reaction, 4 mmol of dry manganese acetate ($Mn(CO_2CH_3)_2$, Aldrich) is added to a mixture containing 15 mL of trioctylamine and 3 g of oleic acid (12 mmol) at room temperature. The resulting mixture is heated rapidly to 320 °C over 10–15 min, and the solution gradually changes to black. The solution is maintained at 320 °C for 1 h under N_2 flow to yield uniform MnO nanocrystals with up to yields of 80%. The nanocrystals are cooled and extracted into hexane by precipitation with ethanol, centrifugation, and redispersion. The nanocrystals were characterized using transmission electron microscopy (TEM, JEOL 100cx, acc. 100 kV) and X-ray powder diffraction (XRD, Scintag X_2). TEM samples were prepared by placing a drop of a dilute hexane dispersion of nanocrystals on the surface of a 400 mesh copper grid backed with Formvar and were dried in a vacuum chamber at 80 °C for 1 h. XRD samples were prepared by drying a dispersion of nanocrystals on a piece of Si (100) wafer. The XRD spectrum (Figure 1) exhibited the highly crystalline peaks that can be matched to the series of Bragg reflections corresponding to the standard and phase pure cubic rock salt structure of MnO ($Fm3m$, $a = 4.442$ Å). The particle size, calculated from the Debye–Scherrer equation, was 6.8 nm, confirmed by average 7 nm diameters in the TEM (Figure 2a). Nanocrystal assembly from hexane solutions into closed packed arrays was also observed, demonstrating the uniformity of the particle size and retention of the oleic acid capping group.
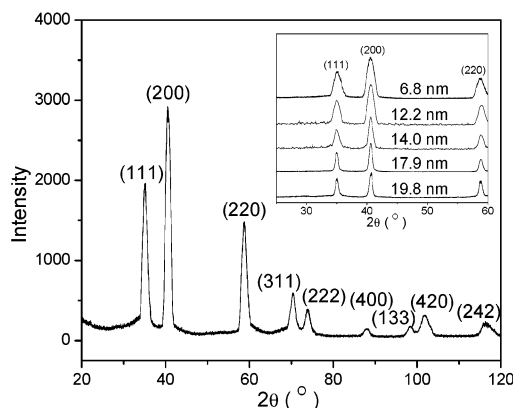

Figure 1. X-ray powder diffraction patterns of 7 nm diameter MnO nanocrystals indexed to the rock salt structure. Inset: X-ray powder diffraction patterns of MnO nanocrystals with average diameters from 6.8 to 19.8 nm (calculated from Debye–Scherrer analysis).
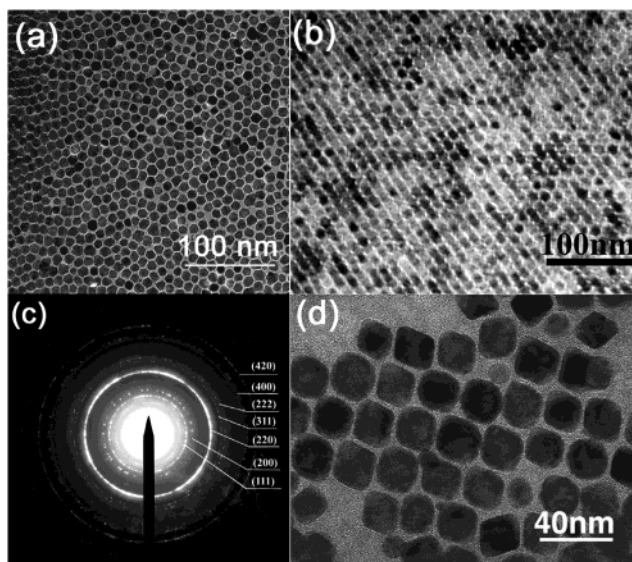

Figure 2. Transmission electron micrographs of (a) 7 nm diameter MnO nanocrystals (monolayer assembly) and (b) 14 nm MnO nanocrystals (multilayer assembly). (c) Selected area electron diffraction pattern of MnO nanocrystals indexed to the rock salt structure. (d) TEM micrograph of 20 nm diameter MnO nanocrystals. Acquired from a JEOL 100cx spectrometer operating at 100 kV.

Controlling evaporation conditions allowed for the formation of a three-dimensional closed-packed superlattice assembly of 14 nm MnO nanocrystals (Figure 2b). Selected area electron diffraction patterns (SAED) of all samples indicate a highly crystalline rock salt structure, in good agreement with XRD (Figure 2c).

To prepare monodisperse 12–20 nm MnO nanoparticles, the same procedure was executed with an additional annealing step:
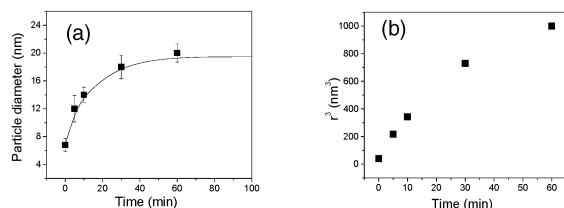
Figure 3. (a) The average diameter of MnO nanocrystals as a function of growth time at 100 °C. (b) Replotted as the particle diameter cubed versus the growth time, in accordance with the LSW model as described in eq 2.

after the temperature was kept at 320 °C for 1 h, the resulting solution was carefully cooled to 100 °C, and nanocrystals with increasing diameter gradually grew at this lower temperature. We were able to follow the average increase in size (from TEM) of MnO nanocrystals with time to prepare samples with average diameters of 12, 14, 18, and 20 nm after 5, 10, 30, and 60 min, respectively (Figure 3a). Selected area electron diffraction patterns confirmed the MnO structure. Particle size was determined and cross-referenced by XRD Debye−Scherrer analysis and TEM. An increase in cubic faceting of the nanocrystals was observed with an increase in size (Figure 2d).

We have employed the Lifshitz−Slyozov−Wagner (LSW) model to further develop a quantitative understanding of the growth kinetics of transition metal oxide nanocrystals.[10−12] Particle growth is driven by the dependence of the solubility of a solid phase on the particle size according to the Gibbs−Thomson equation.[13] Assuming that the particles are spherical, the solubility, c_r, of a particle with radius r is given by

$$c_r = c_\infty \exp\left(\frac{2\gamma V_m}{RT}\frac{1}{r}\right) \qquad (1)$$

where c_∞ is the solubility at a flat surface, γ is the surface energy of the solid, V_m is the molar volume, R is the gas constant, and T is the temperature. For the case where $(2\gamma V_m/rRT) < 1$ such that the exponential term in eq 1 can be linearized, and assuming that the growth rate is determined by diffusion of the solute from the smaller particles to the larger particles, the following rate law is obtained:[10−12]

$$r^3 - r_0^3 = \frac{8\gamma D V_m^2 c_\infty}{9RT} t \qquad (2)$$

where r is the particle radius at time t and r_0 is the particle radius at time zero.[13] Figure 3b shows the cube of particle radius plotted versus time. We can infer from the roughly linear dependence that the increase in particle size is dominated by diffusion-limited growth at this temperature. The intercept at $t = 0$ corresponds to the particle size (7 nm) of the as-prepared sample.

We are currently investigating the ability to extend this experimental procedure to a wider range of binary transition metal oxides. Chemical oxidation of 7 nm MnO nanocrystals with trimethylamine-

N-oxide, following methods akin to that of Hyeon and co-workers,[6] leads to the formation of uniform and ligand-capped 7 nm nanocrystals of Mn_3O_4 (hausmannite structure, $I41/amd$, $a = 5.762$ Å, $c = 9.470$ Å), as characterized by XRD and TEM (see Supporting Information). We were also successful in the preparation of highly uniform 14 nm ligand-capped nanocrystals of FeO (Wuestite structure, $Fm3m$), using the same method by substituting for Fe(II) acetate as the precursor.

In conclusion, we have prepared high-quality MnO nanocrystals with alkyl chain capping groups, and these crystals are stable in nonpolar solvents. The synthetic procedures offer the following advantageous features for the fabrication of transition metal oxide nanocrystals. First, this method is simple and reproducible; the yield of the current process is over 80%. Second, highly crystalline and monodisperse nanocrystals were obtained directly without further size selection. Third, particle size can be easily and fractionally increased by this method enabling kinetic studies. Preliminary magnetic measurements show that the as-synthesized MnO and Mn_3O_4 nanoparticles are superparamagnetic at room temperature.[14]

Supporting Information Available: TEM, selected area electron diffraction pattern and XRD powder pattern of 7 nm diameter Mn_3O_4 nanocrystals, enlarged TEM of the three-dimensional closed-packed MnO superlattice assembly, and TEM of 14 nm diameter cubic FeO nanocrystals (PDF). This material is available free of charge via the Internet at http://pubs.acs.org.

References

(1) (a) Nayak, S. K.; Jena, P. *Phys. Rev. Lett.* **1998**, *81*, 2970. (b) Lidstrom, E.; Hartmann, O. *J. Phys: Condens. Matter* **2000**, *12*, 4969. (c) Pask, J. E.; Singh, D. J.; Mazin, I. I.; Hellberg, C. S.; Kortus, J. *Phys. Rev. B* **2001**, *64*, 024403.
(2) (a) Giraldo, O.; Brock, S. L.; Willis, W. S.; Marquez, M.; Suib, S. L. *J. Am. Chem. Soc.* **2000**, *122*, 9330. (b) Tarascon, J. M.; Armard, M. *Nature* **2001**, *414*, 359.
(3) Solovyev, I. V.; Terakura, K. *Phys. Rev. B* **1998**, *58*, 15496.
(4) Nayak, S. K.; Jena, P. *J. Am. Chem. Soc.* **1999**, *121*, 644.
(5) Lee, G. H.; Huh, S. H.; Jeong, J. W.; Choi, B. J.; Kim, S. K.; Ri, H. C. *J. Am. Chem. Soc.* **2002**, *124*, 12094.
(6) Hyeon, T.; Lee, S. S.; Park, J.; Chung, Y.; Na, H. B. *J. Am. Chem. Soc.* **2001**, *123*, 12798.
(7) Lee, S.; Jun, Y.; Cho, S.; Cheon, J. *J. Am. Chem. Soc.* **2002**, *124*, 11244.
(8) Rockenberger, J.; Scher, E. C.; Alivisatos, A. P. *J. Am. Chem. Soc.* **1999**, *121*, 11595.
(9) (a) Arii, T.; Kishi, A.; Ogawa, M.; Sawada, Y. *Anal. Sci.* **2001**, *17*, 875. (b) Cozzoli, P. D.; Curri, M. L.; Agostiano, A.; Leo, G.; Lomascolo, M. *J. Phys. Chem. B* **2003**, *107*, 4756.
(10) Oskam, G.; Nellore, A.; Penn, R. L.; Searson, P. C. *J. Phys. Chem. B* **2003**, *107*, 1734.
(11) Lifshitz, I. M.; Slyozov, V. V. *J. Phys. Chem. Solids* **1961**, *19*, 35.
(12) Wagner, C. Z. *Elektrochem.* **1961**, *65*, 581.
(13) Peng, X.; Wickham, J.; Alivisatos, A. P. *J. Am. Chem. Soc.* **1998**, *120*, 5343.
(14) Magnetic measurements were carried out with the assistance of Uemero and co-workers on a superconducting quantum interference device with typical fields and temperatures of 2−300 K.

JA0362656